Volume 20, No 3 | International Journal of Radiation Research, July 2022

Preparation, molecular modeling and *in-vivo* evaluation of ^{99m}Tc-Oseltamivir as a tumor diagnostic agent

S.B. Challan[1,2], S.I. Khater[2,3*], A.M. Rashad[4,5]

[1]*Labeled Compounds Department, Hot Lab. Center, Egyptian Atomic Energy Authority, Cairo, Egypt*
[2]*Cyclotron Project, Nuclear Research Center, Egyptian Atomic Energy Authority, Cairo, Egypt*
[3]*Radioactive Isotopes and Generators Department, Hot Lab. Center, Egyptian Atomic Energy Authority, Cairo, Egypt*
[4]*Accelerators and Ion Sources Department, Nuclear Research Center, Egyptian Atomic Energy Authority, Cairo, Egypt*
[5]*Central Laboratory for Elemental and Isotopic Analysis, Nuclear Research Center, Egyptian Atomic Energy Authority, Cairo, Egypt*

► ***Original article***

Corresponding author:
Sabah I. khater, Ph.D.,
E-mail:
sabkhater@yahoo.com

Received: July 2021
Final revised: December 2021
Accepted: February 2022

Int. J. Radiat. Res., July 2022; 20(3): 635-642

DOI: 10.52547/ijrr.20.3.17

Keywords: *Oseltamivir, technetium-99m, spartan, in-vivo biodistrbution.*

ABSTRACT

Background: Radiolabeling process has a very important role in prediction of *in-vivo* biodistribution. Moreover, biodistribution is considered the backbone of the recent discovery of anti-cancer drugs.Technetium-99m has been the most utilized radionuclide in nuclear medicine due to its optimal physical characteristics. ***Materials and Methods***: Oseltamivir(Osel) was radiolabeled by technetium-99m under reductive conditions directly.1.5 mg of Osel was followed by 25 µg of $SnCl_2.H2O$, 200 µl buffer pH 4 at 60ºC reaction temperature, and the reaction time was 30 minutes. I*n-vivo* biodistribution of ^{99m}Tc-Oseltamivir (^{99m}Tc-Osel) tracer was studied using tumor-bearing Albino mice compared to control. The radiochemical purity percentage was calculated using the ascending paper chromatography technique and also, confirmed by paper electrophoresis before the *in-vivo* biodistribution in mice.^{99m}Tc-Osel tracer was further analyzed utilizing high performance liquid chromatography analysis .Spartan software for molecular modeling is used for optimizing the different complex patterns of Osel with ^{99m}Tc where energy was minimized using the semi-empirical method with a PM3 basis set. ***Result***: ^{99m}Tc-Osel tracer was synthesized with a good yield of 98.7±0.34% at the optimized conditions and the preparation exhibited *in-vitro* stability up to 3 h. In vivo biodistribution studies showed high uptake in tumor cells with the target to the non-target ratio of 4.55±0.2 after 3 h. post-injection. ***Conclusion***: ^{99m}Tc-Osel tracer focuses on the tumor site with a high percentage appropriate to use ^{99m}Tc-Osel as a useful tool for tumor imaging.

INTRODUCTION

Oseltamivir (Tamiflu) with a chemical structure as shown in figure 1, is an anti-influenza drug which becomes widely used since the widespread of H1N1 [1]. It is ingested as a tablet consists of Osel phosphate as in active form, which changes over the hepatic esterase into the active form Osel carboxylate [2]. Cancer is the main reason for death worldwide due to its being highly aggressive and associated with a poor prognosis, resistance to drug therapy in some cases, along with high rates of metastasis, as well as it contributes to the decrease survival rates in patients [3].

Since the 1970s, it has been approved as a chemotherapeutic agent. It is considered a novel anti-cancer agent by its mechanism as a Neu1 inhibitor that acts on the cell surface through a receptor level signaling pathway to modulate a number of glycosylated receptors[4]. Osel phosphate offers a possible therapeutic diagnosis for pancreatic and breast cancer [5].

However, most of chemotherapeutics lack good therapeutic index, selectivity and multi-drug resistance [6-8]. It is clear that limitations of the chemotherapeutics are the main rational to generate new and more effective anticancer *agents.*

Studies of the biodistribution are the key components of the modern process of anticancer drug discovery and play a significant role in drug development [9]. Radiolabeling process is one of the tools, which is used to predict *in-vivo* biodistribution of the new drugs.

Recently, there are many radiopharmaceuticals based on, such as radioiodine ($^{123/125}$ I), florin (^{18}F), and technetium-99m (^{99m} Tc) as a new model of tumor imaging-agents [10-12].

Technetium-99m has been the most utilized radionuclide in nuclear medicine due to its optimal physical characteristics (half-life time of 6 h, low emitting gamma scintillation energy of 140 keV, and minimal doses to the patients), convenient

[DOI: 10.52547/ijrr.20.3.17]

availability from the ^{99}Mo / ^{99m}Tc generator [13-14]. The labeled process with ^{99m}Tc depends on the quantity of reducing agent, chiefly as stannous chloride, which is generally utilized for this purpose [15-16].

In the current work, the benefits of radiolabeling in anticancer drugs discovery and development was utilized. Tamiflu was radiolabeled with one of the diagnostic isotopes, ^{99m}Tc, to evaluate its biodistribution and confirm its tumor localization in order to investigate its diagnostic ability.

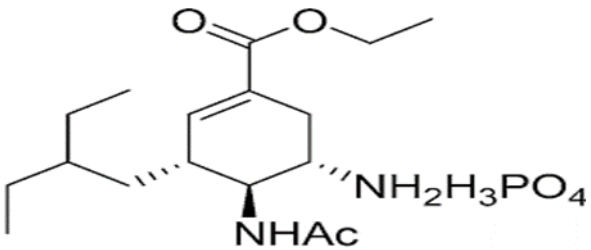

Figure 1. Structure of Oseltamivir phosphate.

MATERIALS AND METHODS

All chemical materials and solvents were purchased from commercial companies and used directly without additional purification. Oseltamivir phosphate, Stannous chloride dihydrate ($SnCl_2.2H_2O$), and Sodium pertechnetate (Na $^{99m}TcO_4$) were obtained from commercial ^{99}Mo/ ^{99m}Tc generator (Radioisotope Production Facility, Egyptian Atomic Energy Authority). For sterility filtration, 22- µm diameter Millipore filter was used. Paper electrophoresis (PE) instrument was provided by E.C. Apparatus Corporation, power supply (300 V) and chamber unit, USA. An HPLC instrument with UV spectrophotometer detector model SpD-6A, Reversed phase Lischorosorb (RP-C18) column (25 cm × 4.6 mm, 5 µl) associated with a γ-beam scintillation counter model Scalar Ratemeter SR 7 model, (Nuclear Enterprises Ltd., USA).

Labeling procedure

Oseltamivir was labeled by technetium-99m under reductive conditions using stannous chloride dihydrate directly [17].The reaction mixture was performed in an evacuated penicillin vial to assess the optimal condition for labeling. Different values of Osel (0.5-3 mg) were diluted in 0.5 ml of purged-nitrogen distilled water, followed by (5-200 µg) stannous chloride solution, 0.2 ml of different reaction medium pH solutions (2-11) were added. Finally, about 0.1 ml of ^{99m}Tc-pertechnetate freshly eluted from the molybdenum generator producing 7.2 MBq was added to each vial, vortex thoroughly and the reaction mixture was incubated for 5-60 min at temperatures 25-100 ºC.

Quality control of ^{99m}Tc-Oseltamivir

The reaction mixture *was analyzed* after labeling of Osel with ^{99m}Tc *by TLC, Electrophoresis*, and reverse-phase HPLC before *in-vivo* biodistribution in mice [18-19].

TLC was performed on silica gel using two mobile phase, acetone and the mixture solution was obtained from ammonium hydroxide: ethanol: water: (1:2:5 v:v:v). A sample from the reaction mixture was spotted on the TLC strip, then free $^{99m}TcO_4^-$ was determined using acetone as a mobile phase. In this case, free $^{99m}TcO_4^-$ moved to the solvent front (*Rf*= 1), whereas ^{99m}Tc-Osel and colloid remained at the point of spotting. The colloid amount (reduced hydrolyzed technetium) was estimated utilizing a mixture solution. In this case, reduced hydrolyzed technetium remains at the start point (*Rf* = 0), whereas other species migrated to the top solvent front (*Rf*= 1). After complete development, the strips were dried and cut into 1 cm pieces, and measured by γ-counter. The radiochemical yield percentage was calculated by subtracting the total amount of reduced hydrolyzed technetium and free pertechnetate from 100% [20, 21].

In electrophoresis analysis

The radiochemical purity yield of ^{99m}Tc-Osel was assessed using cellulose acetate strips to confirm the TLC result. These strips were moistened with 0.9 NaCl solution then, introduced into the chamber. A solution of ^{99m}Tc-Osel was filtrated through a 0.22 µm Millipore filter for eliminating the colloidal impurities, if present, and then, 5 µl of each sample was applied at a distance of 6 cm from the cathode. The samples were kept for 1.5 h at 300 volts. The strips were removed, and cut into 1 cm segments, then counted with gamma counter. The radiochemical yield percentage was calculated as the quantity of the radioactivity of the labeled product at segment zero after subtracting the quantity of the radioactivity of the free technetium at segment 10 to the total radioactivity multiplied by 100 [22,23].

In HPLC analysis

An amount of about 20 µL of reaction sample was injected on a RP-18 column using a gradient of mobile phase A (aqueous solution of 50 mM potassium dihydrogen orthophosphate at pH=3.5) and mobile phase B (acetonitrile), (50:50 v/v) at a flow rate of 1ml/min at ambient temperature and wave length = 254 nm .. Each 0.5 mL fraction was collected using a fraction collector and counted in a well type gamma-counter [24].

In-vitro stability

Stability of the labeled compound was evaluated in fresh serum and phosphate buffer saline (PBS) at various time intervals: 0.5, 1, 2, 3, 4, and 24 hours. A volume of 100 µl (200 µci) of^{99m}Tc-oseltamivir tracer

[DOI: 10.52547/ijrr.20.3.17]

was incubated at 37ºC with 1ml of fresh human serum and (PBS), pH=7.4. Afterword, 5 µl of this mixture was taken at different time intervals up to 24 h for analysis by TLC method [25].

Animal studies

Animal experiments were performed in compliance with the guidelines established by Animal ethics committee, Labeled Compounds Department, Egyptian Atomic Energy Authority (Ethical approval EAEA/2019/188). It was also in agreement with the rules of the British Animal Protection (BAP). Swiss albino female mice approximately 8-10 weeks of age and weighing 20-30 g, were obtained from the Animal House, Biology Department, EAEA, in Cairo, Egypt. The animals were kept upping at consistent nourishing conditions, all through the trial time and kept at room temperature (22 ± 2 °C) with a 12 h on/ off light schedule. Female mice were utilized due to their tendency to Ehrlich ascites carcinoma risen above that of the male mice. The mice were bred in a cage with a free diet and water [26].

Induction of solid tumor

Ehrlich Ascites Carcinoma (EAC) derived from a murine mammary carcinoma was brought to induce solid tumor. EAC tumor line was brought from the National Cancer Institute, Cairo, Egypt. The EAC parent tumor line was diluted with a biological solution that was sterile. 200 µL (~12.5×10^6 cells/ml) of EAC solution was intramuscular injections into the right thigh of female Albino mice for the induction of a solid tumor and left to grow for a week [27].

In-vivo evaluation studies

In-vivo, evaluation studies were performed using two groups of animals, one group of normal and the other of solid tumors bearing mice, n=7. The mice were injected with 0.1 ml (50-100 MBq) of ^{99m}Tc-oseltamivir tracer mixture into its tail vein after purification with 0.22 µm Millipore filter to eliminate colloidal impurities [28]. The mice were anesthetized with chloroform and sacrificed after (0.5, 1, 2 and 3 hours) post-injection. Various organs and tissues were dissected, washed with saline, dried, weighed, and counted for radioactivity. Blood, bone, and muscle samples of mice were determined based on their percentage of the total weight of mice 7, 10 and 40, respectively [29, 30]. A correction was made for the background radiation and physical decay during the experiment [31]. Data were expressed as the percentage of injection dose per gram of tissue (% ID/g). The final results were expressed as the mean ± one standard error [32].

Statistical analysis

Graph Pad Prism version 6.0 software was used to do all the statistical analysis. Statistical analysis was conducted using one-way analysis of variance (ANOVA). The results showed that $P < 0.05$ which is considered statistically significant and all the outcomes were given as mean ± SD.

RESULTS

The formation of ^{99m}Tc-Osel tracer depended on the amount of the substrate content, stannous chloride dihydrate content, pH, reaction temperature, and reaction time to provide a high radiochemical purity value. The maximum radiochemical percentage of 98.7±0.34% was obtained from 1.5 mg Osel and 25 µg stannous chloride. The reaction was achieved at 60 ºC for 30 min at a pH of 4 (figures 2-6).

Influence of Osel content is shows in figure 2. A low radiochemical yield was obtained (89±1.2 %) at 0.5 mg Osel while by increasing the amount of Osel to 1.5 mg, the optimum radiochemical yield (94.5±1.1 %) was obtained.

Influence of stannous chloride dihydrate content ($SnCl_2.2H_2O$) is illustrated in figure 3. At a low amount of $SnCl_2.2H_2O$ (5 µg), the radiochemical yield of ^{99m}Tc-oseltamivir was 78.3±1.3%. Further increasing of the amount of the stannous chloride dihydrate to 25 µg, led to obtaining the optimum radiochemical yield (95.5±1.1%). When adding an excess stannous chloride dihydrate, the yield was decreased (60±1.3% at 200 µg), and the colloid amount increased to reach 38.5±0.8%.

Influence of pH is shown in figure 4. The ^{99m}Tc-Osel radiolabeling yield was studied at a pH from 2 to 11. As the results revealed, the radiolabeling yield of ^{99m}Tc-oseltamivir was equal to 90.2±0.8 % at pH value of 2. The optimum radiochemical yield was obtained at 95.2±0.7% at pH value of 4. Further increasing the pH value led to decreasing the radiochemical yield to 35.5±0.8% at a pH value of 11.

The influence of reaction time on the radiolabeling yield of ^{99m}Tc- Osel is illustrated in figure 5. The radiochemical yield increases with time till reaching 95.5±1.0% at 30 min. Further increase in the reaction time above 30 min., the radiochemical yield remains constant. The influence of reaction temperature on the radiolabeling yield of ^{99m}Tc- Osel is illustrated in figur 6. The reaction was performed at 25 °C, 40, 60, 80, and 100 °C. The radiolabeling yield of ^{99m}Tc- Osel tracer was increased by increasing temperature until reaching the optimum value (98.7±0.8%) at 60 °C then; remained constant.

In vitro stability of ^{99m}Tc- Osel in human serum and phosphate-buffered saline (PBS) are revealed in figure 7. The stability decreased in serum from 93.5±0.5 to 91.5±0.6 % (~2%), while in the case of PBS, the stability decreased from 91±0.4% to 88±0.3 % (~3%) after 3 hours. The stability of ^{99m}Tc-Osel reached 87.1±0.4%, 76.5±0.6%, respectively, in serum and PBS at 24 h.

[DOI: 10.52547/ijrr.20.3.17]

Quality control of ^{99m}Tc- Osel is illustrated in figure 8 which presents the electrophoresis pattern (about 97.5±1.1%), and in the HPLC technique (about 98.7±1.0%).

Spartan software for molecular modeling is used for optimizing the different complex patterns of Osel with ^{99m}Tc where energy was minimized using the semi-empirical method with a PM3 basis set as shown in figure (10). Complexes A–E represent coordination manner between two molecules of Osel with one atom of technetium, while complex F represents coordination manner between one molecule of Osel with one atom of technetium.

In vivo bioevaluation study of ^{99m}Tc- Osel in normal mice is shown in table 1. The results showed that ^{99m}Tc-oseltamivir tracer was distributed rapidly in the blood to reach 8.57±0.06% at 0.5 h. post injection (p.i) and cleared easily until reaching 1.9±0.01% after 3 h. post injection (p.i.) as shown in figure 13. The data also showed that ^{99m}Tc-Osel was easily distributed in the liver, kidney, stomach and intestine at 0.5 h post-injection. After 1 h post-injection, a high concentration of ^{99m}Tc-osel tracer has been found in the liver stomach, intestine and kidney to reach 2.4±0.05 %, 8.97±0.17%, 5.33±0.2% and 40.1±1.2%, respectively.

In vivo evaluation study of ^{99m}Tc- Osel in solid tumor bearing mice is shown in table 2. The results showed that ^{99m}Tc-osel tracer was distributed rapidly in the blood to reach 7.1±0.09% at 0.5 h. p.i and cleared easily until reaching1.18±0.06 % after 3 h. p.i. as shown in figure 11. Studying the bioevaluation of ^{99m}Tc-osel tracer revealed that ^{99m}Tc-osel tracer was accumulated rapidly in the liver, kidney, stomach and intestine at 1 h. p.i. to reach 3.74±0.12%, 22.8±0.5%, 5.45±0.27% and 4.47±0.3%, respectively, and decreased with time. The uptake of ^{99m}Tc- Osel tracer in the solid tumor tissue right thigh target (T) inoculated with EAC into normal tissue left thigh non target (NT) and reached ratio of 4.55 at 3 h. p.i.

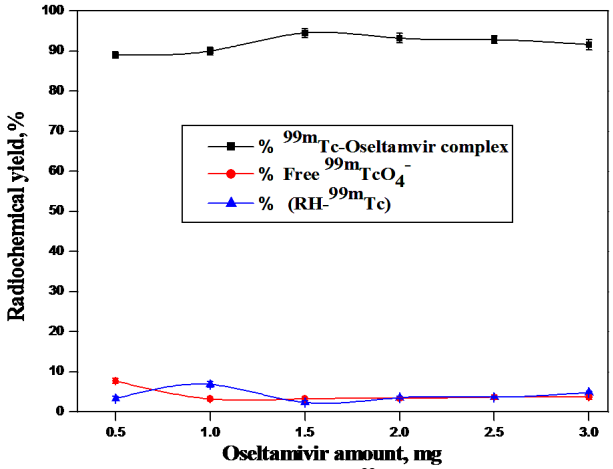

Figure 2. Radiochemical yield of ^{99m}Tc-Osel versus Osel amount. X mg of Osel, 25 µg of $SnCl_2.2H_2O$, 100µL of ^{99m}TcO4- solution (7.2 MBq), pH 4, at room temperature for 30 min.

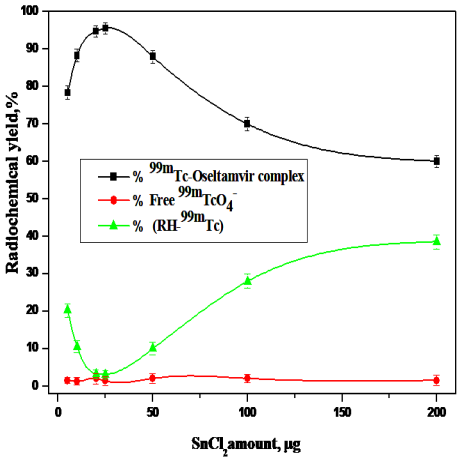

Figure 3. Radiochemical yield of ^{99m}Tc-Osel as a function of $SnCl_2.2H_2O$ amount. Reaction conditions: 1.5 mg of Osel, x µg $SnCl_2.2H_2O$ solution, 100µL of ^{99m}TcO4- solution (7.2 MBq), pH 4, the reaction mixture was kept at room temperature for 30 min.

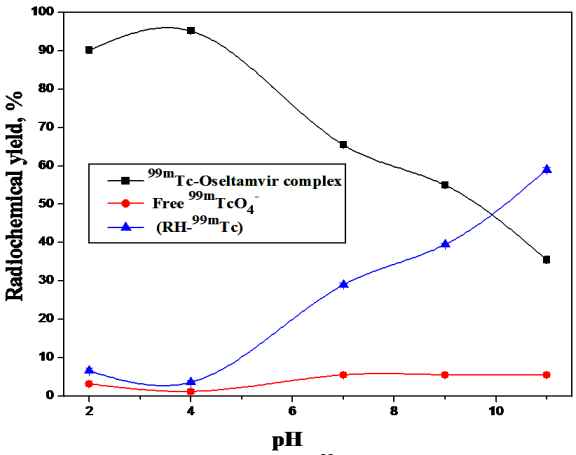

Figure 4. Radiolabeling yield of ^{99m}Tc-Osel versus reaction pH.1.5 mg of Osel, 25µg $SnCl_2.2H_2O$, and100L of ^{99m}TcO4- solution (7.2 MBq), 200 µL buffer of different pH (2-11) the reaction mixture was kept at room temperature for 30 min.

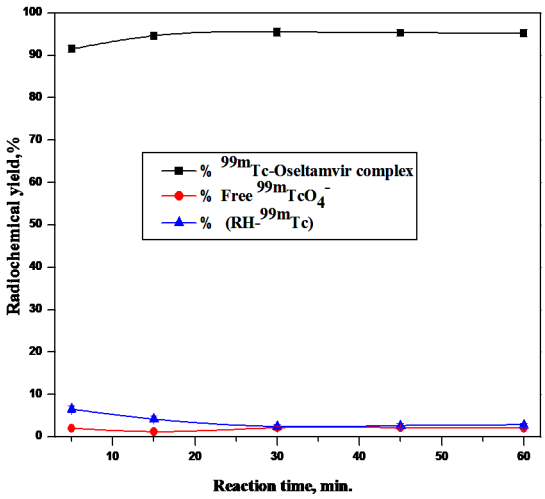

Figure 5. Radiolabeling yield of ^{99m}Tc-Osel versus the reaction time.1.5 mg of Osel, 25 µg $SnCl_2.2H_2O$, and 100µL of activity (7.2 MBq), at pH 4, the reaction mixture was kept at room temperature with different time intervals.

[DOI: 10.52547/ijrr.20.3.17]

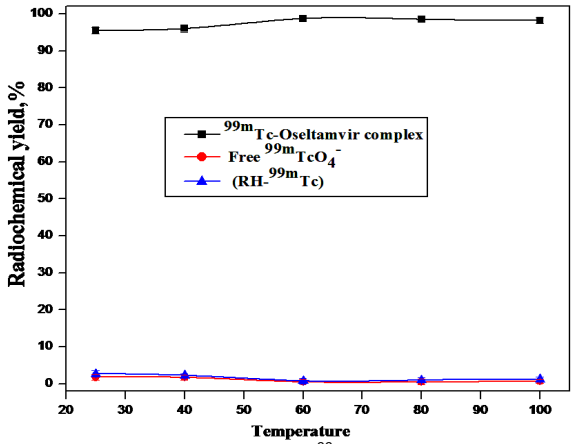

Figure 6. Radiolabeling yield of ^{99m}Tc-Osel versus reaction temperature.1.5 mg of Osel, 25 µg $SnCl_2.2H_2O$, and 100µL of ^{99m}TcO4- solution (7.2 MBq), at pH 4, the reaction mixture was kept at different temperature for 30 min.

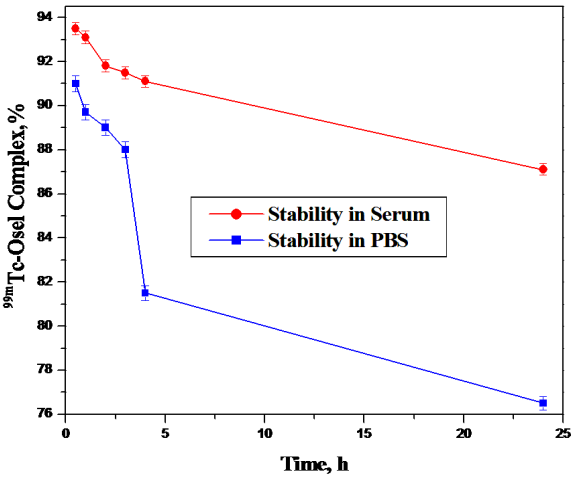

Figure 7. Stability of ^{99m}Tc-Osel tracer in fresh serum and PBS with time *in-vitro*.

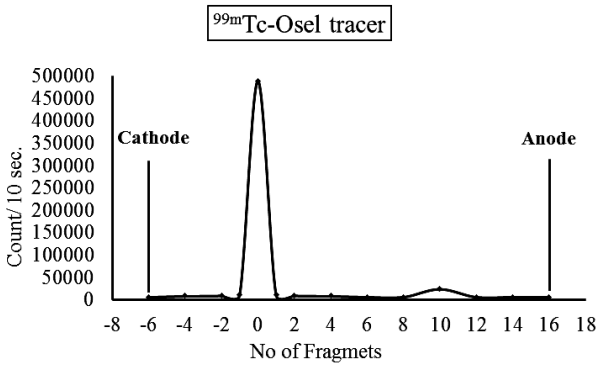

Figure 8. Electrophoresis radiochromatogram of ^{99m}Tc-Osel tracer.

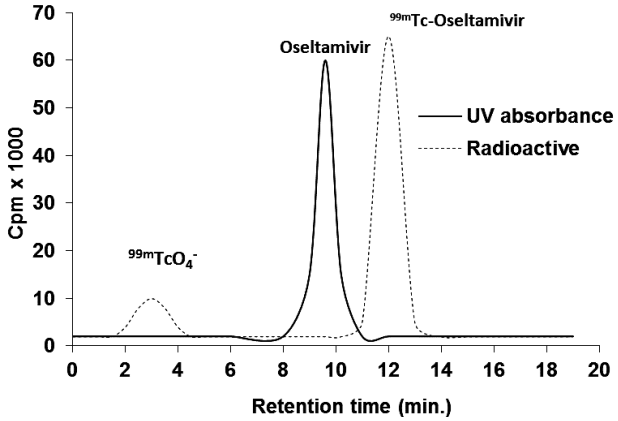

Figure 9. HPLC radiochromatogram of free technetium-99m (TcO_4^-) and ^{99m}Tc-Osel(^{99m}Tc-Osel) were given at Rt of 3 and 12 min, respectively, HPLC-UV radiochromatogram of Oseltamivir was given at Rt = 9.6 min.

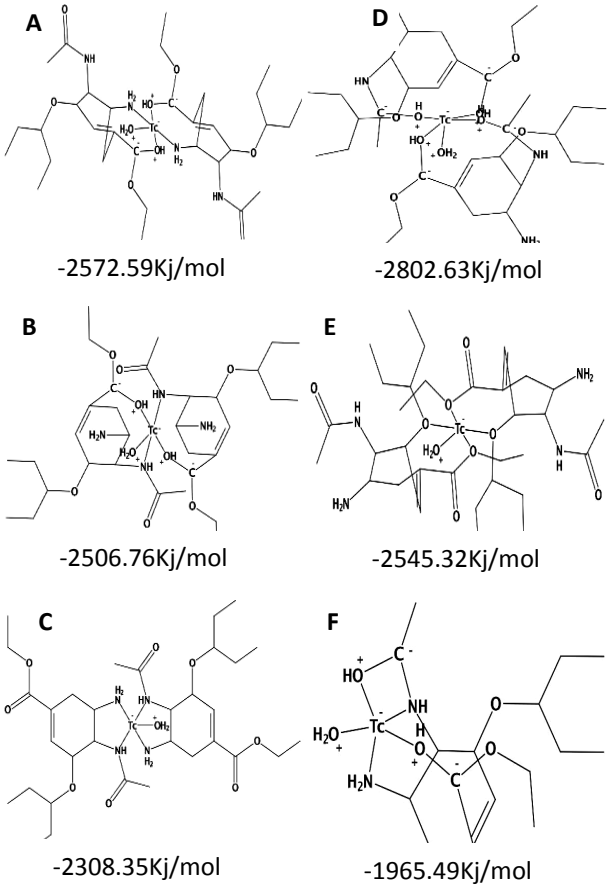

Figure 10. Optimized structures of the proposed ^{99m}Tc-Oseltamivir tracer and their energies*. *Complexes A–E represent coordination manner between two molecules of Oseltamivir with one atom of technetium, F represents coordination manner between one molecule of Oseltamivir with one atom of technetium.

[DOI: 10.52547/ijrr.20.3.17]

Table 1. Bio-distribution of ^{99m}Tc-Oseltamivir in normal mice as %ID/g tissue. Values are expressed as mean ± SD, n = 7.

Organs/ Tissues	ID/g tissue (%)			
	Time post injection (h.)			
	0.5 h.	1 h.	2 h.	3 h.
Blood	8.57±0.06	3.47±0.04	2.1±0.02	1.9±0.01
Bone	3.46±0.05	3.76±0.07	3.23±0.04	1.2±0.04
Muscles	1.28±0.03	1.77±0.04	0.98±0.06	0.39±0.02
Brain	0.27±0.06	0.25±0.07	0.24±0.04	0.22±0.02
Stomach	1.88±0.9	8.97±0.17	1.56±0.08	1.37±0.03
Intestine	1.46±0.09	5.33±0.2	3.15±0.11	3.1±0.09
Kidney	23.8±0.7	40.1±1.2	12.1±0.9	9.89±0.9
Liver	2.1±0.04	2.4±0.05	1.75±0.04	1.39±0.03
Spleen	1.75±0.08	1.14±0.09	0.94±0.06	0.79±0.05
Lung	4.75±0.1	1.47±0.09	1.32±0.09	0.76±0.07
Heart	5.27±0.08	1.81±0.07	1.11±0.05	0.57±0.04
Urine	17.6±1.1	51.3±1.5	46±1.3	61.5±1.6

Table 2. Bio-distribution of 99mTc-Oseltamivir in solid tumor bearing mice as %ID/g tissue. Values are expressed as mean ± SD, n = 7.

Organs/Tissues	ID/g tissue (%)			
	Time post injection (h.)			
	0.5 h.	1 h.	2 h.	3 h.
Blood	7.1±0.09	2.95 ±0.07	1.48±0.05	1.18±0.06
Bone	2.59±0.06	3.11±0.07	2.48±0.05	0.73±0.04
Muscles (Control) (NT)	1.12±0.02	1.34±0.03	1.29±0.03	0.82±0.01
Muscles (Tumor) (T)	1.48±0.02	2.11±0.03	4.47±0.04	3.73±0.05
Brain	0.38±0.02	0.31±0.02	0.28±0.01	0.21±0.01
Stomach	2.18±0.12	5.45±0.27	3.3±0.18	0.98±0.1
Intestine	2.37±0.28	4.47±0.3	1.34±0.25	0.49±0.1
Kidney	10.6±0.4	22.8±0.5	12.1±0.3	11.1±0.3
Liver	2.79±0.14	3.74±0.12	2.57±0.11	1.98±0.1
Spleen	2.4±0.11	1.33±0.1	1.1±0.09	0.91±0.05
Lung	4.3±0.12	1.61±0.11	1.57±0.1	1.39±0.09
Heart	3.37±0.15	1.59±0.12	1.39±0.11	1.1±0.07
Urine	6.3±0.32	65±0.58	18±0.26	29.6±0.37
T/NT	**1.32**	**1.57**	**3.46**	**4.55**

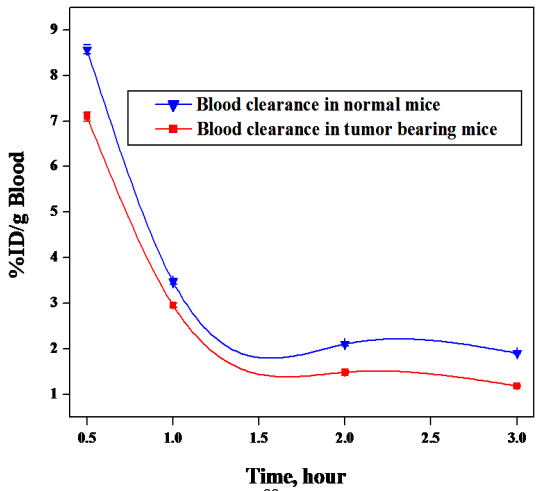

Figure 11. Blood clearance of ^{99m}Tc-Osel tracer in normal and tumor mice verses time.

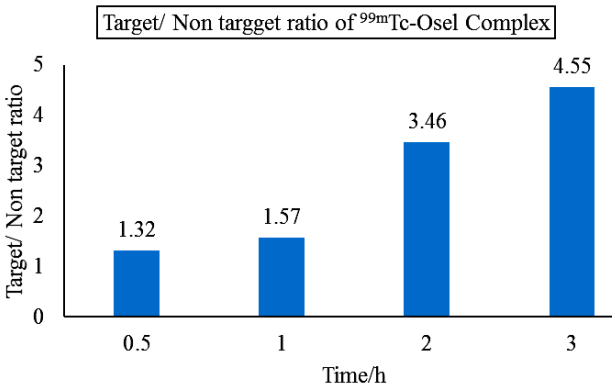

Figure 12. Ratio of target (T) / non target (NT) muscle by ^{99m}Tc-Osel tracer verses time.

DISCUSSION

The radiochemical yield of the complex strongly depend on the amount of the ligand. The optimum radiochemical yield was obtained at 1.5 mg Osel. Below this amount, the radiochemical yield decreased because the Osel amount was insufficient to form the complex with the whole amount of the reduced technetium. Further increasing in the ligand amount did not change the labeling yield noticeably.

A low amount of $SnCl_2.2H_2O$, gives a low radiochemical yield probably because these amounts were insufficient for reducing the whole amount of pertechnetate. A higher amount of $SnCl_2.2H_2O$ over 25 µg also led to a decrease in the radiochemical yield of the complex with increasing the colloidal stannic oxide species. This may be due to the fact that the Osel became conjugated with technetium-99m Thus, in the absence of Osel, free pertechnetate was reduced to non-soluble technetium TcO_2-xH_2O (colloid) [33-5].

The pH of the reaction medium was considered a very critical point in the percentage of the labeling yield. The optimum radiochemical yield was obtained at pH value of 4. A further increase in the pH value results in decreasing the radiochemical yield. This may be attributed to the fact that stannous chloride dihydrate promptly precipitates the formation of free $^{99m}TcO_4^-$ and non-soluble reduced ^{99m}Tc colloid in an alkaline medium [36, 37].

The radiochemical yield increases with time till reaching 30 min. By continuous increasing of the reaction time (above 30 min.) the radiochemical yield remains constant. This means that ^{99m}Tc-Osel tracer is stable at the higher temperature.

In vitro stability of ^{99m}Tc-Osel was higher in human serum than in phosphate-buffered saline (PBS) as shown in figure 7. Consequently, ^{99m}Tc- Osel tracer has a good stability in serum and in PBS[38,39].

The electrophoresis pattern of ^{99m}Tc-Osel revealed that ^{99m}Tc-Oseltracer remains close to the

[DOI: 10.52547/ijrr.20.3.17]

spotting point (about 97.5±1.1%) which confirmed the TLC result. while free pertechnetate pushes toward the anode to separate at 10 cm from the spotting point.

^{99m}Tc- Osel tracer was further analyzed by high performance liquid chromatography analysis as shown in figure 9. The most energetically favored proposed complex was D because it has the lowest energy value (*E* = -2802.63 kJ/mol).

The results of *in-vivo* bioevaluation studies showed that ^{99m}Tc-Oseltracer was distributed rapidly in the blood at 0.5 h. (p.i) and significantly decreased at 3 h. p.i. The data showed that^{99m}Tc-Osel easily distributed in the liver, kidney, stomach and intestine at 0.5 h post-injection. After 1 h post-injection, a high concentration of ^{99m}Tc-Osel tracer has been founded in the liver stomach, intestine and kidney, respectively.

The rapid presence of ^{99m}Tc-Osel tracer in the liver may be due to the extensive conversion of Osel to active metabolite Osel carboxylate by the hepatic esterase located in the liver. This study indicates that ^{99m}Tc-Osel showed significant hydrophilic characteristics due to its being rapidly cleared by glomerular filtration tubules in the kidney after 1 h of injection. The most likely excretion route for ^{99m}Tc- Osel and its metabolites were through the kidneys and bladder [40].The results revealed that the distribution of ^{99m}Tc- Osel in the brain is generally limited during all time intervals. The majority of organs, tissues showed a significant decrease in the ^{99m}Tc-Osel tracer uptake with time. In vivo localization of ^{99m}Tc-Osel tracer showed that the target-to-non-target muscle ratio increased over time to reach a ratio of 4.55 after 3 h post injection, as shown in figure 12.

The present study indicates that ^{99m}Tc-Osel showed a significant hydrophilic characteristics. It quickly reached the target area and was rapidly cleared by glomerular filtration tubules in the kidney after 1 h of injection. The newly synthesized ^{99m}Tc-Osel complex showed higher uptake in solid tumor cells (about 3.46, 4.55, respectively, at 2h, 3h. p.i.) based on target to non-target ratio more than the recently published SPECT tracers such as, ^{99m}Tc (CO) 3-labeled chlorambucil analog (3.2 at 3 h. ^{99m}Tc-DMSAme (2.49 at 2 h), ^{99m}Tc-sunitinib (3 at 1 h), and ^{99m}Tc-Luteolin (0.94 at 3 h) [41-44]. According to the results of the *in-vivo* bioevaluation studies, the synthesized ^{99m}Tc-Osel complex showed a high tumor sites uptake with a good retention time suitable for tumor imaging. These promising characteristics make ^{99m}Tc-Oselcomplex as a suitable candidate for diagnosis of solid tumors. The ^{99m}Tc-Osel complex affords a beneficial radiopharmaceutical of high tumor uptake and good retention time sufficient for imaging the tumor.

CONCLUSION

A newly synthesized ^{99m}Tc-Osel complex was perfectly prepared via direct labeling technique with a maximum yield of 98.7±0.34% at optimum condition and *in-vitro* stability up to 7 h. The biological evaluation of ^{99m}Tc-Osel complex showed a high accumulation ratio of ^{99m}Tc-Osel complex in solid tumor target (T) compared to non-target (NT) (about 4.55 at 3 h. p.i.). Thus, it may be concluded that ^{99m}Tc-Osel tracer can be used as a useful tumor imaging diagnostic agent for preclinical studies.

ACKNOWLEDGEMENTS

The authors would like to acknowledge Dr. Mohamed El-desawy, Nuclear Research Center, Egyptian Atomic Energy Authority, Cairo, Egypt, for his contribution in study.

Funding: This research did not receive any specific grant from funding agencies in the public, commercial or not-for-profit sectors.

Conflict of interest: The authors declare that they have no conflicts of interest to disclose.

Ethical considerations: Animal experiments were performed in compliance with the guidelines established by Animal ethics committee, Labeled Compounds Department, Egyptian Atomic Energy Authority (Ethical approval EAEA/2019/188).

Author contribution: Safaa B. Challan: Methodology, Data curation, Writing - original draft. S. I. Khater: Visualization, Investigation, Resources. A. M. Rashad: Validation, Theoretical calculations, Writing - review & editing.

REFERENCES

1. Schunemann HJ, Hill SR, Kakad M, Bellamy R, Uyeki TM, Hayden FG (2007) WHO Rapid Advice Guidelines for pharmacological management of sporadic human infection with avian influenza A (H5N1) virus. *The Lancet Infectious Diseases, **7**(1): 21–31*.
2. Ward P, Small I, Smith J, Suter P, Dutkowski R (2005) Oseltamivir (Tamiflu) and its potential for use in the event of an influenza pandemic. *Journal of Antimicrobial Chemotherapy, **55**: (S1, i5–i21)*.
3. Reddy LH, Sharma RK, Murthy RS, (2004) Enhanced tumour uptake of doxorubicin loaded poly (butyl cyanoacrylate) nanoparticles in mice bearing Dalton's lymphoma tumour. *J Drug Target, **12**: 443–451*.
4. Amin AM, El-Azony KM, Ibrahim IT (2009) Application of ^{99}Mo/^{99m}Tc alumina generator in the labeling of metoprolol for diagnostic purposes. *J Labell Compd Radiopharm, **52**: 467-472*.
5. Wilson JC and von Itzstein M (2003) Recent strategies in the search for new anti-influenza therapies. *Current Drug Targets, **4**(5):3 89–408. PMID: 12816348*.
6. Seddon BM and Workman P (2003) The role of functional and molecular imaging in cancer drug discovery and development. *Br J Radiol, **76**(2): S128-38*.
7. Chidambaram M, Manavalan R, KathiresanK (2011) Nanotherapeutics to overcome conventional cancer chemotherapy limitations. *J Pharm PharmSci, **14**(1): 67-77*.
8. Garraway LA and Janne PA (2012) Circumventing cancer drug resistance in the era of personalized medicine. *Cancer Discov, **2**(3):*

[DOI: 10.52547/ijrr.20.3.17]

214-26.
9. Cunningham VJ, Parker CA, Rabiner EA, Gee AD, Gunn RN (2005) PET studies in drug development: methodological considerations. *Drug Discov Today Technol, **2**: 311–5*.
10. Rischin D, Hicks RJ, Fisher R, Binns D, Corry J, Porceddu S, Peters LJ (2006) Trans-Tasman radiation oncology group study 98.02. Prognostic significance of (^{18}F)-misonidazole positron emission tomography-detected tumor hypoxia in patients with advanced head and neck cancer randomly assigned to chemoradiation with or without tirapazamine: a sub study of Trans-Tasman Radiation Oncology Group Study 98.02. *J ClinOncol, **24**(13): 2098-104*.
11. Altiparmak B, Lambrecht FY, Bayrak E, Durkan K, (2010) Design and synthesis of ^{99m}Tc-citro-folate for use as a tumor targeted radiopharmaceutical. *Int J Pharm, **400**(1-2): 8–14.*
12. Stypinski D, McQuarrie SA, McEwan AJB, Wiebe LI (2018) Pharmacokinetics and scintigraphic imaging of the hypoxia imaging agent (^{123}I) IAZA in healthy adults following exercise based cardiac stress. *Pharmaceutics **10**: 25*.
13. Hesselewwod S and Leubg E (1994) Drug interactions with radiopharmaceuticals. *Eur J Nucl Med, **21**: 348*.
14. Early PJ and Sodee DB (1995) Principles and practice of nuclear medicine. Mosby- Year Book, Inc., Toronto, 877.
15. Saha GB (1998) Fundamentals of nuclear pharmacy. *Springer-Verlag, New York, pp.: 331*.
16. Sampson CB., (1996), Complications and difficulties in radiolabelling blood cells: a review. *Nucl Med Commun, **17**(8): 648-58*.
17. Richardson VJ, Jeyasingh K, Jewkes RF (1977), Properties of ^{99m}Technetium labeled liposomes innormal and tumor bearing rats. *BiochemSoc Trans, **5**: 290-291*.
18. Cheng CH, Meares CF, Godwin DA (1983) Application of nuclear and radiochemistry, Lambrecht, R.M. and Morcos, N., Eds., New York: Pergamon.
19. Abd El-Ghany EA (1998) Preparation and evaluation of freeze dried kits for ^{99m}Tc labeling, *M.Sc. Thesis*, Faculty of Pharmacy, Cairo Univ. (Egypt).
20. Gandomkar M, Najafi R, Mazidi M, Mirfallah SH, Goudarzi M (2009) Three different procedures in labeling of Ubiquicidin with technetium 99m: a comparative study. *Int J Radiat Res, **7**(2): 97-104*.
21. Massoud A, Safaa BC, Maziad N (2021) Characterization of polyvinylpyrrolidone (PVP) with technetium-99m and its accumulation in mice**.** Part a: *Journal of Macromolecular Science, Pure and Applied Chemistry, **58**(6): 408–418*.
22. Challan SB and Massoud A (2017) Radiolabeling of grapheme oxide by Technetium-99m for infection imaging in rats. *J Radioanal Nucl Chem, **314**(3): 2189*.
23. Challan SB, Fawzy AM, Massoud A (2020) Synthesis of radioiodinatedcarnosine for hepatotoxicity imaging induced by carbon tetrachloride and its biological assessment in rats. *Radiochem Acta, **108**: 397-408*.
24. Ibrahim T, Walyb MA, El-Tawoosy M (2012) Synthesis, Labeling, and Biological Evaluation of 2-{(Benzyl (cyanomethyl) amino) methyl}-3-(ethoxycarbonyl)-quinoxaline 1,4-Dioxide in Ascites Bearing Mice. *Radiochemistry, **54**(4): 395–40*.
25. Nagarajan JSK and Muralidharan S (2009) A validated RP-HPLC method for estimation of Oseltamivir in pharmaceutical formulation. *Der Pharmacia Lettre, **1**(1): 162-168*.
26. Motaleb MA, Farouk N, El-Kolaly MT, *et al.* (2007) Synthesis of 99m Tc-L-carnitine as a model for tumor imaging.
27. *Arab J Nucl SciAppl, **40**(2): 101*.
28. NDong C, Tate JA, Kett WC, Batra J, Demidenko E, Lewis LD, Hoopes PJ, Gerngross TU, Griswold KE (2015) Tumor cell targeting by iron oxide nanoparticles is dominated by different factors *In-vitro* versus *In-vivo*. *plos one, **10**(2): 1-18*.
29. Jagetia GC and Rao SK (2006) Evaluation of antineoplastic activity Guduchi (Tinosporacordifolia) in Ehrlich Ascites Carcinoma bearing mice. *Biological and Pharmaceutical Bulletin, **29**: 460-66*.
30. Konan YN, Cerny R, Favet J, Berton M, Gurny R, Allemann E (2003) Preparation and characterization of sterile sub-200 nm meso-tetra (4-hydroxylphenyl)porphyrin-loaded nanoparticles for photodynamic therapy. *Eur J Pharm Biopharm, **55**: 115-124*.
31. Nour SA, Abdelmalak NS, Naguib MJ, Rashed HM, Ibrahim AB (2016) Intranasal brain-targeted clonazepam polymeric micelles for immediate control of status epilepticus: *In-vitro* optimization, ex vivo determination of cytotoxicity, in vivo biodistribution and pharmacodynamics studies. *Drug Deliv, **23**: 3681-3695*.
32. Mohamed KO, Nissan YM, El-Malah AA, Ahmed WA, Ibrahim DM, Sakr TM, Motaleb MA (2017) Design, Synthesis and Biological Evaluation of Some Novel Sulfonamide Serivatives as Apoptotic Agents. *Eur J Med Chem, **135**: 424-433*.
33. Breeman WA, Hofland LJ, Bakker WH, van der Pluij M, Van Koetsveld PM, de Jong M, Setyono-Han B, Kwekkeboom DJ, Visser TJ, Lamberts SW, Krenning EP (1993) Radioiodinatedsomatostatin analogue RC-160: preparation, biological activity, *in-vivo* application in rats and comparison with (^{123}I-Tyr3)octreotide. *Eur J Nucl Med, **20**: 1089–1094*.
34. Al-wabli RI, Sakr, TM, Khedr MA, Adli ASA, Motaleb MA, Zaghary WA (2016) Platelet-12 lipoxygenase targeting via newly synthesized curcumin derivative radiolabeled with technetium-99m. *Chem Cent J, **10**: 73*.
35. Tubergen K, Corlija M, VolkertWA, Holmes RA (1991) Sensitivity of technetium- 99m-d, 1-HMPAO to radiolysis in aqueous solutions. *J Nucl Med, **32**: 111-115*.
36. Motaleb MA, Ibrahem IT, Ayoub VR, Geneidi AS (2016) Preparation and biological evaluation of ^{99m}Tc–ropinirole as a novel radiopharmaceutical for brain imaging. *J Label CompdRadiopharm, **59**: 147–152*.
37. Geskovski N, Kuzmanovska S, Simonoska Crcarevska M, Calis S, Dimchevska S, Petrusevska M, Zdravkovski P, Goracinova K (2013) Comparative biodistribution studies of technetium-99 m radiolabeled amphiphilic nanoparticles using three different reducing agents during the labeling procedure. *J Labelled Comp Radiopharm, **56**(14): 689-95*.
38. Sanad MH, Farouk N, Fouzy ASM (2017) Radiocomplexation and bioevaluation of 99mTc nitrido-piracetam as a model for brain imaging. *Radiochimica Acta, **105**(9): 729-737*.
39. Sanad MH, El-Bayoumy ASA, Ibrahim AA (2017) Comparative biological evaluation between 99mTc (CO) 3 and 99mTc-Sn (II) complexes of novel quinoline derivative: a promising infection radiotracer. *J RadioanalNucl Chem, **311**: 1-14*.
40. Srivastava SC and Richards P (1983) Technetium-labled compounds. In Radiotracers for Medical Applications, CRC Series in Radiotracers in Biolology and Medicine, 1st ed.; Rayudu, G.V.S., Ed.; CRC Press: Boca Raton, FL, USA.
41. Sakr TM, Khedr MA, Rashed HM, Mohamed ME (2018) In Silico-Based Repositioning of Phosphinothricin as a Novel Technetium-99m Imaging Probe with Potential Anti-Cancer Activity. *Molecules, **23**: 496*.
42. Satpati D, Korde A, Venkatesh M, Banerjee S (2009) Preparation and bioevaluation of a 99mTc-labeled chlorambucil analog as a tumor targeting agent. *Appl Radiat Isot, **67**: 1644-1649*.
43. Zhang J, Yu Q, Huo J, Pang Y, Yang S, He Y, Tang T, Yang C, Wang X (2010), Synthesis and biodistribution of a novel ^{99m}Tc-DMSA metronidazole ester as a potential tumor hypoxia imaging agent. *J Radioanal Nucl Chem, **283**: 481-485*.
44. Sakr TM, El-Safoury DM, Awad GAS, Motaleb MA (2013) Biodistribution of ^{99m}Tc-sunitinib as a potential radiotracer for tumor hypoxia imaging. *J Label Compd Radiopharm, **56**: 392–395*.
45. El-Sharawy DM, Khater SI, Essam HM, Noheir HS, Hossam MH, Elmaidomy AH (2021) ^{99m}Tc-Luteolin: Radiolabeling, *In Silico* ADMET and Biological Evaluation as a Natural Tracer Tumor imaging. *J Radiat Res and Appl Sci, **14**(1): 125-132*.

[DOI: 10.52547/ijrr.20.3.17]